Available online at www.sciencedirect.com
SCIENCE DIRECT®
Journal of the European Ceramic Society 25 (2005) 433–439
www.elsevier.com/locate/jeurceramsoc

Synthesis and characterisation of $La(Co_{1/2}Ti_{1/2})O_3$

D. L. Cairns [a,*], I. M. Reaney [a], H. Zheng [a], D. Iddles [b], T. Price [b]

[a] *Department of Engineering Materials, Mappin Street, Sheffield, South Yorkshire S1 3JD, UK*
[b] *Filtronic Comtek, Enterprise Drive, Station Road, Four Ashes, Wolverhampton WV10 7DB, UK*

Received 28 July 2003; received in revised form 24 February 2004; accepted 28 February 2004
Available online 4 June 2004

Abstract

Single phase, dense $La(Co_{1/2}Ti_{1/2})O_3$ (LCT) ceramics have been fabricated using conventional solid state synthesis. Samples were investigated using X-ray diffraction (XRD), transmission electron microscopy (TEM), Raman spectroscopy and their dielectric properties were studied at radio and microwave frequencies. X-ray and electron diffraction conclusively revealed that LCT contained in-phase and antiphase rotations of the O-octahedra, consistent with and $a^-a^-c^+$ tilt system in the Glazer classification. However, XRD indicated that the Co and Ti ions were disordered on the B-site whereas TEM and Raman spectroscopy exhibited reflections and modes which suggested that partial ordering may be present. Moreover, some Raman bands could only be explained by assuming that at least some of the octahedra exhibited a Jahn–Teller distortion. Dielectric measurements indicated that LCT is insulating with low dielectric loss, 0.0024 at 1 MHz and frequency independent relative permittivity, $\varepsilon_r = 25$. A quality factor, $Q \times f_o = 38{,}000$ was obtained at microwave frequencies along with a temperature coefficient of the resonant frequency, TCF $= -42\,MK^{-1}$.

Keywords: $La(Co,Ti)O_3$; Dielectric properties; Defects; X-ray methods; Electron microscopy

1. Introduction

Ln-based complex perovskites, e.g. $La(Mg_{1/2}Ti_{1/2})O_3$ (LMT) have a negative temperature coefficient of resonant frequency (TCF $\sim -50\,MK^{-1}$) and a permittivity (ε_r) ~ 25.[1] They may be combined with positive TCF materials, e.g. $CaTiO_3$, $+850\,MK^{-1}$, to produce microwave dielectric ceramics with a TCF tuneable through zero.[1] Commercial compounds, often based on $La(Zn_{1/2}Ti_{1/2})O_3$, are insulating and highly selective to specific resonant frequencies defined by a large value of microwave dielectric quality factor, $Q \times f_o \approx 30{,}000$ GHz. However, the formation and dielectric properties of $La(Co_{1/2}Ti_{1/2})O_3$ (LCT) and $La(Ni_{1/2}Ti_{1/2})O_3$ (LNT) ceramics have not been investigated in detail. Recently, the crystal structure of LCT and LNT were studied by Rodriguez et al.[2] At room temperature the compound had an $a^-a^-c^+$ tilt system with $\sqrt{2}a_p \times \sqrt{2}a_p \times 2a_p$ unit cell in which the B-site ions were partially ordered in a rocksalt superlattice, giving a monoclinic space group $P2_1/n$[2] as illustrated in Fig. 1.

At room temperature, perovskite $LaCoO_3$ adopts R-3c symmetry with an $a^-a^-a^-$ tilt system, according to Glazer notation[3] but the structure, electronic and magnetic properties of this material have remained the subject of controversy and debate since the initial studies of this compound over 40 years ago.[4,5] The temperature dependence of the magnetic susceptibility of $LaCoO_3$ shows two transitions occurring at approximately 100 and 500 K, initially interpreted by Goodenough[5] as evidence for a spin state transition. However, neutron powder diffraction studies have failed to provide evidence for an order–disorder transition at ~500 K in $LaCoO_3$, which should be accompanied by a change in space group from R-3c to R-3.[6,7] In addition, air-fired, $LaCoO_3$ is usually semiconducting due to the presence of O vacancies which are related to a reduction of Co^{3+} to Co^{2+}.[8] In contrast, air-fired, $La_{2/3}TiO_3$ has an $a^-a^-c^+$ tilt system and adopts orthorhombic symmetry, *Pnma*, and is highly insulating with $\varepsilon_r = 69$, $Qf_0 = 17{,}000$ GHz and TCF $= 20\,MK^{-1}$. It is not stable in its pure form but small additions of, e.g., Sr^{2+} on the A–site or Al^{3+} on the B-site, leads to single phase material.[9,10]

It is the intention of this paper to describe the formation of dense, LCT ceramics using a conventional solid state synthesis route. Its structure and dielectric properties at radio

* Corresponding author.
E-mail address: mtq01dc@sheffield.ac.uk (D.L. Cairns).

0955-2219/$ – see front matter © 2004 Elsevier Ltd. All rights reserved.
doi:10.1016/j.jeurceramsoc.2004.02.016

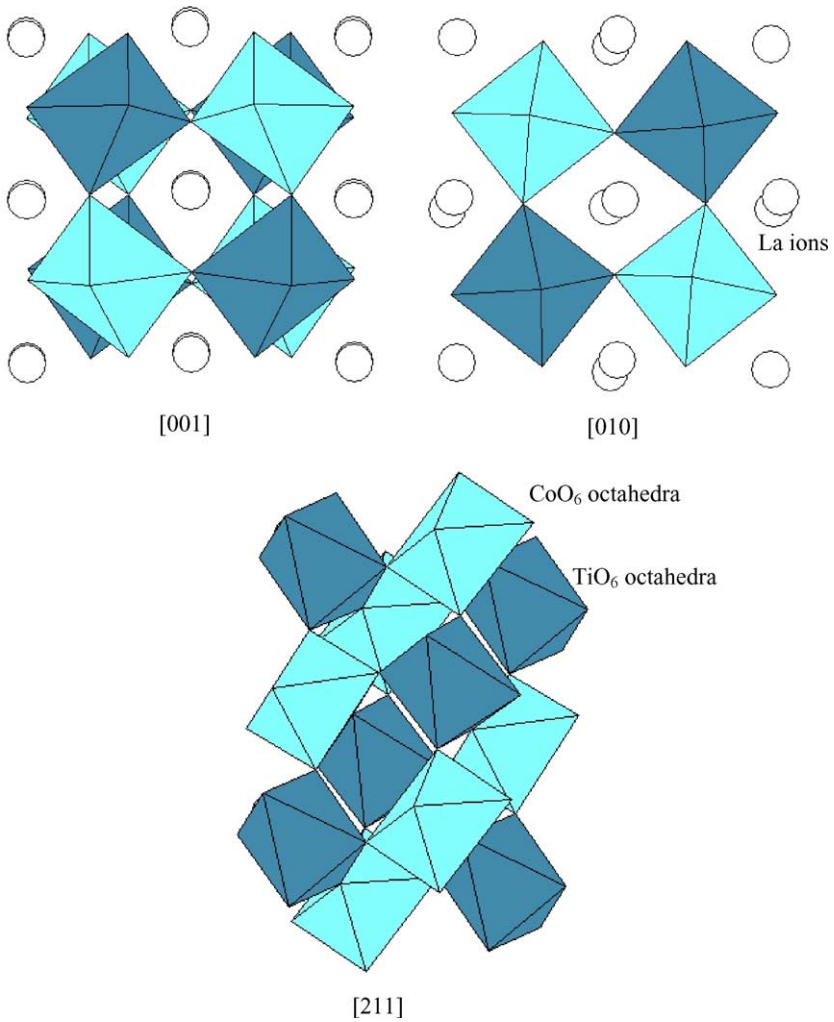

Fig. 1. (a) [0 0 1], (b) [0 1 0], and (c) [2 1 1] pseudocubic projections of ordered LCT ($P2_1/n$) based on ionic positions suggested by Rodriguez et al.[2] The images show the in-phase tilting, antiphase tilting of the octahedra along with ordering of the B-site species, respectively.

and microwave frequencies are studied to establish whether it is a useful end member in the fabrication of solid solutions intended for microwave dielectric applications.

2. Experimental

Ceramics were synthesised by a conventional mixed oxide route using, TiO_2, La_2O_3 and $CoCO_3$ (acros organics). The chemical purity of all these raw starting materials was >99%. The weighed starting reagents, in appropriate ratios, were ball-milled to a 1 μm mean particle size, Laser Coulter Analyser, in propan-2-ol for 16 h, using ZrO_2 media. The slurry was dried and then calcined 6 h at 1350 °C. The calcined powder was re-milled for 16 h, then pressed into discs. Discs were sintered 6 h on ZrO_2 boards at a temperature of 1550 °C. All the fired samples have relative densities above 96% of the theoretical value.

An X-ray diffractometer (Model PW 1730/10 Philips, Holland) with Cu Kα source ($\lambda = 1.540562$ Å), operated at 50 kV and 30 mA, was used for the identification of phases. A step size of 0.02°, a scan rate of 2°/min and scan ranges of 10–70° were adopted. Samples for scanning electron microscopy (SEM) were obtained from fracture surfaces of the sintered pellets. Samples were then mounted on stainless steel stubs using silver dag and carbon-coated. A JEOL JSM6400 SEM equipped with a LINK energy dispersive X-ray (EDS) detector and ancillary electronics operating at 20 kV was used to obtain secondary electron images. Samples for transmission electron microscopy (TEM) were ground to approximately 20 μm thick after which a Cu support ring with an 800 μm circular hole was glued onto its surface. Samples were then thinned on a Gatan Duo Mill ion beam thinner operating at an accelerating voltage of 6 kV and a combined gun current of 0.6 mA at an incidence angle of 15°. TEM was carried out on a Phillips EM420 operating at 120 kV.

A Renishaw Ramascope System 2000 spectrometer was used for Raman measurements. This system comprised an integral Raman microscope, a stigmatic single spectrograph

and a Peltier-cooled charge channel display detector. The microscope attachment was an Olympus BH2 system and the excitation wavelength used was 633 nm from a He-Ne laser source. Power of 1–3 mW was incident on the samples in a 2 μm diameter spot through a standard 50× microscope objective lens. The spectra were collected with 30 s data point acquisition time, a spectral range of 150–950 cm^{-1} and a spectral resolution of 3–4 cm^{-1}. Raman spectra were analysed using GRAMS/AI V.7, which is a fully interactive data processing package including peak-fitting, data smoothing, quantitative analysis, peak picking, and integration for Raman spectrum analysis. Spectra were then presented as relative intensity (counts) versus Raman shift (cm^{-1} in air).

Sintered discs were ground flat and parallel using 1200 grit SiC paper. Pt paste was then brushed onto both flat surfaces and fired at 900 °C for 1 h. Impedance spectroscopy was carried out at room temperature using a HP 4192A impedance analyser measuring in the frequency range 5 Hz to 13 MHz. A DC voltage of 100 mV was applied and the data were corrected for sample geometry.

Microwave measurements (ε_r, Q and TCF) were performed using a silver plated aluminium cavity >∼4 times the diameter of the test resonator (this ensured an "isolated" but shielded resonator) and an Agilent vector network analyser (8753ES) with a range from 30 kHz to 6 GHz. Samples were located at the centre of the cavity on a 99.5% alumina support, thus avoiding any influence from the metallic cavity walls. Microwave energy was coupled to the test piece using a single probe, measuring in reflectance. After calibration for the cables and cavity, the coupling was adjusted such that losses were lower than −30 dB. Q is approximated using Eq. (1):

$$Q = \frac{f_o}{BW} \quad (1)$$

where f_o is the resonant frequency and BW is the bandwidth measured at 7 dB from the resonant peak minimum. Measurement of Q was at ambient temperature and the resonance mode measured was $TE_{0\,1\delta}$. TCF measurements were performed in the same aluminium cavity placed inside a Tenney temperature control cabinet. Resonant frequency measurements were performed at 60, 20 and −10 °C when the $TE_{0\,1\delta}$ mode was stable. TCF was calculated using Eq. (2):

$$TCF = \frac{f_{60} - f_{-10}}{f_{20} \times 70} \quad (2)$$

where f_{60} is the resonant frequency at 60 °C, f_{-10} is the resonant frequency at −10 °C and f_{20} is the resonant frequency at 20 °C.

3. Results and discussion

3.1. X-ray diffraction (XRD)

Fig. 2 shows the X-ray diffractogram obtained from sintered LCT. Only two peaks could not be indexed according

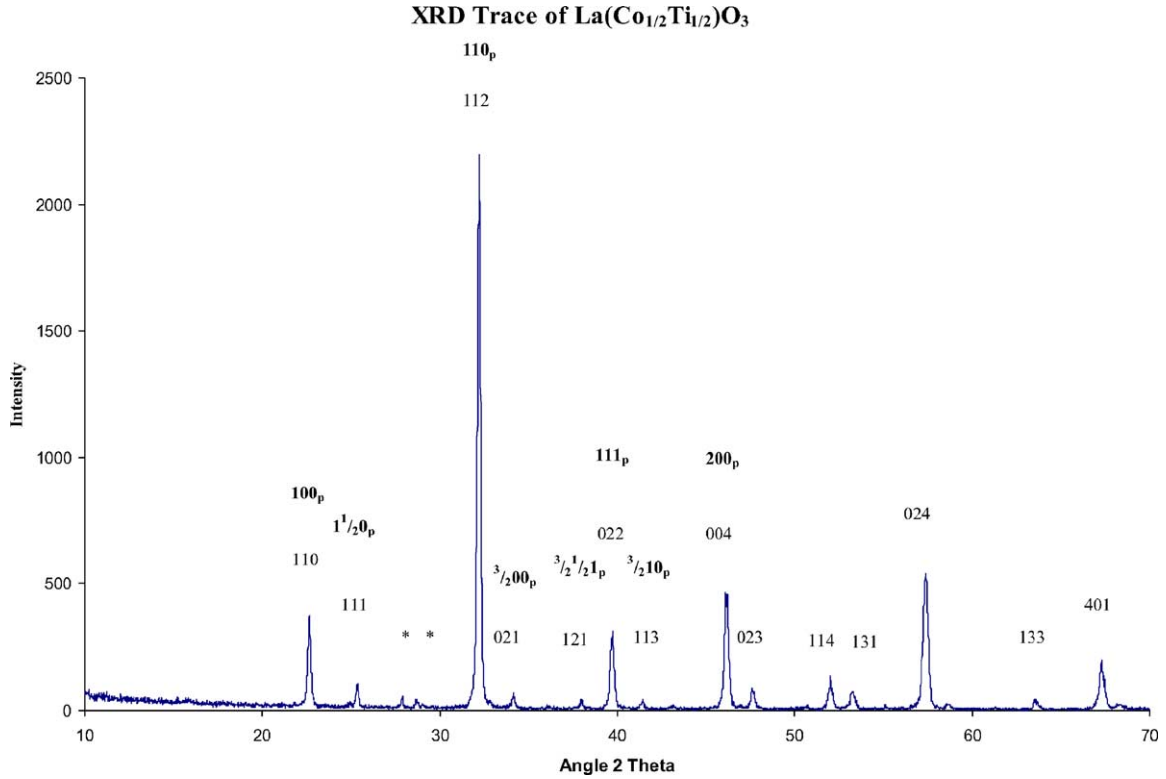

Fig. 2. X ray diffractogram of as-calcined $La(Co_{1/2}Ti_{1/2})O_3$ (LCT). The peaks are indexed using an orthorhombic and pseudocubic setting (bold).

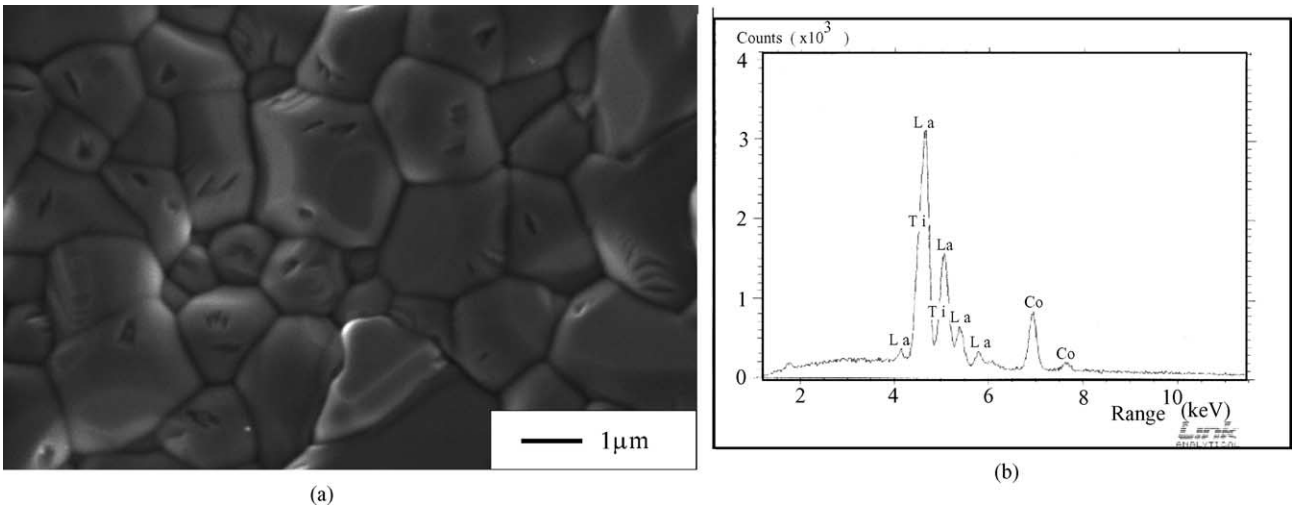

Fig. 3. (a) Secondary electron SEM image and (b) EDS trace for LCT.

to an orthorhombic cell (*Pbnm*, $a = 5.66$ Å, $b = 5.58$ Å, $c = 7.87$ Å), (*), and are attributed to ZrO_2, present due to contamination from the milling media. The *Pbnm* cell is associated with an $a^-a^-c^+$ tilt system which in a pseudocubic setting gives rise to superlattice reflections at 0.5 integer positions.[3] These are indicated in bold in Fig. 2 along with the fundamental perovskite peaks. In LMT, Mg and Ti ions form an ordered rocksalt superlattice that gives rise to reflections at all $1/2\{h\,k\,l\}_p$ positions.[1] Reflections arising from antiphase rotations of the O-octahedra are coincident with the rocksalt superlattice reflections but are only permitted when $h \neq k = l$ (or equivalent).[3] Therefore, unique ordering reflections occur at 0.5 integer positions for which $h = k = l$ (e.g. $1/2\{1\,1\,1\}_p$). These are absent in Fig. 1. However, Ti and Co are close together in the periodic table so the scattering length difference is small and the $1/2\{1\,1\,1\}_p$ peaks may be difficult to resolve.

3.2. Scanning electron microscopy (SEM)

Fig. 3a and b show the SEM micrograph and EDS trace of LCT, respectively. The grain size of LCT is ~2 μm and there is little porosity consistent with a measured density 96% of theoretical. There is no evidence of second phase and EDS shows only the expected elements, La, Ti and Co in the appropriate ratios.

3.3. Transmission electron microscopy (TEM)

Fig. 4 shows the domain variance of electron diffraction patterns in the three major pseudocubic zone axes: (Fig. 4a and b) $\langle 0\,0\,1\rangle_p$; (Fig. 4c and d) $\langle 0\,1\,1\rangle_p$; and (Fig. 4e) $\langle 1\,1\,1\rangle_p$. The fundamental spots (strong) are indexed according to the simple perovskite cell. Superlattice reflections are present in all patterns at half integer positions. $1/2\{h\,k\,l\}_p$ (circled) arise either from rotations of the octahedra in antiphase or rocksalt ordering of the Co and Ti ions. $1/2\{h\,k\,0\}_p$ (square) arise from in phase rotations and $1/2\{h\,0\,0\}$(arrowed) arise from antiparallel cation displacements.[3,11] All reflections are consistent with an $a^-a^-c^+$ tilt system which gives rise to either *Pbnm* (disordered Co/Ti ions) or $P2_1/n$ (ordered) space group symmetry.[1,3,11] Dark field (DF) images obtained using a $1/2\{h\,0\,0\}$ reflection reveal planar defects with ribbon like morphology, Fig. 5, typical of APBs and similar to those observed in $CaTiO_3$.

Unique reflections associated with rocksalt superlattice are difficult to identify unambiguously by electron diffraction because of dynamical double diffraction,[11] e.g.

$$\tfrac{1}{2}\{3\,1\,1\}_p + \{\bar{1}\,0\,0\}_p = \tfrac{1}{2}\{1\,1\,1\}_p$$

However, the $\langle 1\,1\,0\rangle_p$ variant shown in Fig. 4c, should not contain any $1/2\{h\,k\,l\}$ reflections associated with antiphase rotations of the O-octahedra, providing the tilt system is $a^-a^-c^+$.[12] The presence of these reflections therefore suggests that LCT is ordered, consistent with previous structural refinements.[2]

3.4. Raman spectroscopy and dielectric properties

Raman spectroscopy, is a powerful tool for qualitative understanding of the degree of order in perovskite compounds.[13] In the Raman spectrum of LCT, shown in Fig. 6, 10 scattering bands, centred at 186, 248, 292, 351, 425, 439, 523, 605, 650 and 715 cm^{-1}, are observed. The band at 186 cm^{-1} may be assigned to the mode mainly related to the motion of La^{3+} ions. The lines at 248, 292 and 351 cm^{-1} are assigned to rotation-like modes. The 523 cm^{-1} band most likely results from the internal vibration of the oxygen cage. The frequencies of these peaks fit well with the prediction for an orthorhombic cell. However, the band at 715 cm^{-1} is associated with the "breathing" (A_{1g}) mode of the oxygen octahedra. This mode is only

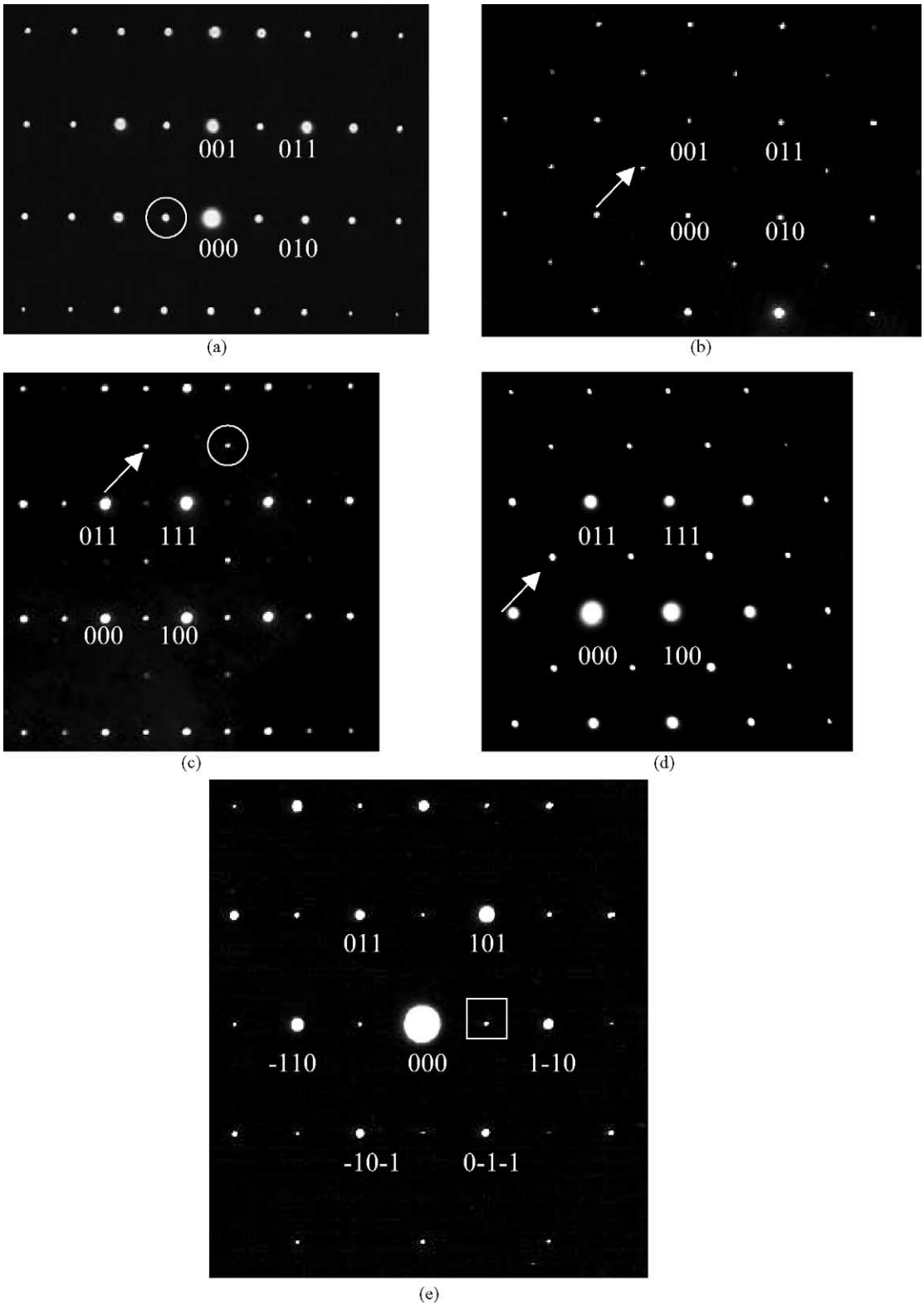

Fig. 4. Domain variance of electron diffraction patterns in the three major pseudocubic zone axes: (a and b) ⟨0 0 1⟩, (c and d) ⟨0 1 1⟩ and (e and f) ⟨1 1 1⟩. Spots are indexed in a pseudocubic setting.

Fig. 5. Dark field (DF) image obtained using a $1/2\{h\,0\,0\}$ reflection revealing planar defects with ribbon like morphology (APBs) (arrowed).

Raman active when neighbouring octahedra are occupied by ions of different valence/size. For ordered complex perovskites such as $BaZn_{1/3}Ta_{2/3}O_3$ (BZT), the peak is sharp and is accompanied by a second band associated with ordering at $\sim$390 cm^{-1}.[14] In general, the peak at $\sim$390 cm^{-1} is sensitive only to long range order (LRO) and is absent or weak in BZT quenched from above the order disorder phase transition temperature ($\sim$1600 °C).[15] In contrast, the band associated with the A_{1g} breathing mode remains present but broadens when LRO is destroyed. This indicates that the band is sensitive to both short- and long-range order, the former characterised by a broad peak the latter by a sharp intensity. In LCT, the breadth of the peak at 715 cm^{-1} and the absence of a strong band around $\sim$380 cm^{-1} suggests at least a short range ordered distribution of Co and Ti ions.[14] However, Raman intensities are difficult to interpret and the LRO band at $\sim$380 cm^{-1} may be weak and obscured by the background. Electron diffraction data suggest that LCT is ordered and Raman data indicate that it is at least short range ordered. Therefore, on balance, it may be concluded that the data presented above are consistent with that presented by the Rodriguez et al.[2] who suggested that, LCT is 'partially ordered'.

Although many bands may be explained by considering that LCT has either an orthorhombic or monoclinic structure, two strong bands occur at 605 and 650 cm^{-1} not specifically assigned to these symmetries. The intensities are strong and their wavenumbers suggest that they may arise from the Jahn–Teller (JT) octahedral distortions associated with the presence of Co^{3+} (high spin) ions in the O-octahedra.[16] The presence of valence states other than Co^{2+} may account for the presence of partial[2] rather than full ordering of the B-site cations. Despite the probable presence of mixed Co ion valence states, the compound remains highly insulating at room temperature with $\varepsilon_r = 25$, TCF $= -42$ MK^{-1} and $Q \times f_o \sim$ 38,000 GHz at microwave frequencies. At lower frequencies (1 MHz), ε_r remains 25 and the dielectric loss is 0.0024.

The above work suggests that LCT (negative TCF) may be a useful end member to form 0 TCF materials with compounds such as Ca, Sr and $BaTiO_3$ (positive TCF) for MW dielectric applications.

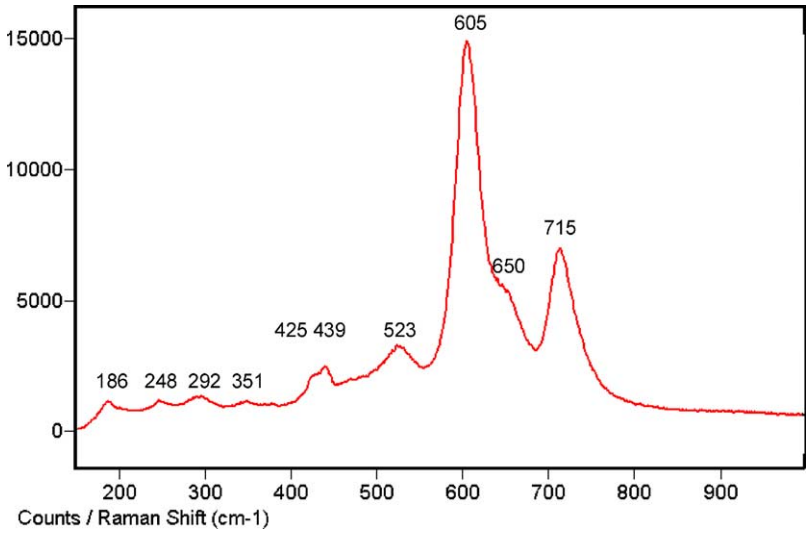

Fig. 6. Raman spectra for LCT.

4. Conclusions

XRD and SEM have shown that dense, ceramic LCT has been successfully fabricated with only minor ZrO_2 contamination from the milling media. Superlattice reflections in XRD and electron diffraction patterns are consistent with an $a^-a^-c^+$ tilt system. Electron diffraction patterns from $\langle 1\,1\,0\rangle$ domain variants suggests that LCT is ordered and Raman spectroscopy indicates that the Co and Ti ions are at least short range ordered, consistent with Rodriguez et al.[2] However, there is evidence of Co^{3+} in high spin configuration since there are bands associated with a unique JT octahedral stretching mode. Dielectric measurements show that LCT is highly insulating with a low dielectric loss at microwave ($Q \times f_o = 38{,}000\,\text{GHz}$) and radio (0.0024) frequencies.

Acknowledgements

The authors would like to thank Dr. P. Korgul and Mr. H. Bagshaw for help with electron microscopy.

References

1. Lee, D. Y., Yoon, S. J., Yeo, J. H., Nahm, S., Paik, J. H. and Whang, K. C., Crystal structure and microwave dielectric properties of $La(Mg_{1/2}Ti_{1/2})O_3$ ceramics. *J. Mater. Sci. Lett.* 2000, **19**(2), 131–134.
2. Rodriguez, E., Lopez, M. L., Campo, J., Veiga, M. L. and Pico, C., Crystal and magnetic structure of the perovskites La_2MTiO_6 (M = Co, Ni). *J. Mater. Chem.* 2002, **12**, 2798–2802.
3. Glazer, A. M., Simple ways of determining perovskite structures. *Acta Cryst.* 1975, **A31**, 756–762.
4. Koehler, W. C., *J. Phys. Chem. Solids* 1957, **2**, 100.
5. Goodenough, J. B., *J. Phys. Chem. Solids* 1958, **10**, 287.
6. Thornton, G., Tofield, B. C. and Williams, D. E., Spin state equilibria and the semiconductor to metal transition of $LaCoO_3$. *Solid State Commun.* 1982, **44**(8), 1213–1216.
7. Thornton, G., Tofield, B. C. and Hewat, A. W., A neutron-diffraction study of $LaCoO_3$ in the temperature-range 4.2-K less-than *T* less-than 1248-K. *J. Solid State Chem.* 1986, **61**(3), 301–307.
8. Senarisrodriguez, M. A. and Goodenough, J. B., $LaCoO_3$ revisited. *J. Solid State Chem.* 1995, **116**(2), 224–231.
9. Houivet, D., El Fallah, J., Bernard, J., Roulland, F. and Haussonne, J. M., Microwave properties and microstructures of $La_{2/3}TiO_3$ stabilized with NiO. *J. Eur. Ceram. Soc.* 2001, **21**(10/11), 1715–1718.
10. Yashima, M., Ali, R. and Yoshioka, H., High-temperature X-ray diffraction study of the lanthanum aluminium titanate perovskite $La_{0.683}Ti_{0.95}Al_{0.05}O_3$. *Solid State Ionics* 2000, **128**(1–4), 105–110.
11. Reaney, I. M., Colla, E. L. and Setter, N., Dielectric and structural characteristics of Ba-based and Sr-based complex perovskites as a function of tolerance factor. *Jpn. J. Appl. Phys. Part 1: Regular Papers Short Notes Rev. Papers* 1994, **33**(7A), 3984–3990.
12. Levin, I., Chan, J. Y., Maslar, J. E., Vanderah, T. A. and Bell, S. M., Phase transitions and microwave dielectric properties in the perovskite-like $Ca(Al_{0.5}Nb_{0.5})O_3$-$CaTiO_3$ system. *J. Appl. Phy.* 2001, **90**(2), 904–914.
13. Iliev, M. N. and Abrashev, M. V., Raman phonons and Raman Jahn–Teller bands in perovskite-like manganites. *J. Raman Spectrosc.* 2001, **32**(10), 805–811.
14. Webb, S. J., Breeze, J., Scott, R. I., Cannell, D. S., Iddles, D. M. and Alford, N. M., Raman spectroscopic study of gallium-doped Ba(Zn1/3Ta2/3)O-3. *J. Am. Ceram. Soc.* 2002, **85**(7), 1753–1756.
15. Qazi, I., Reaney, I. M. and Lee, W. E., Order-disorder phase transition in Ba(Zn1/3Ta2/3)O-3. *J. Eur. Ceram. Soc.* 2001, **21**(15), 2613–2616.
16. Loa, I. *et al*., Pressure-induced quenching of the Jahn–Teller distortion and insulator-to-metal transition in $LaMnO_3$. Phys. Rev. Lett. 2001, **8712**(12), p. art. no. 125501.